Chemistry of *C*-Trimethylsilyl-Substituted Heterocarboranes. 23. Synthetic, Spectroscopic, and Structural Investigation on Half- and Full-Sandwich Magnesacarboranes of 2,3- and 2,4-C_2B_4 Carborane Ligands

Narayan S. Hosmane,*,† Dunming Zhu, James E. McDonald, Hongming Zhang, John A. Maguire, Thomas G. Gray, and Sarah C. Helfert

Department of Chemistry, Southern Methodist University, Dallas, Texas 75275

Received December 19, 1997

The reaction of *nido*-1-Na(L)$_n$-2-(SiMe$_3$)-3-(R)-2,3-$C_2B_4H_5$ (n = 2, L = THF, R = SiMe$_3$; n = 1, L = TMEDA, R = SiMe$_3$ or Me) or *closo-exo*-5,6-[(μ-H)$_2$Li(L)$_n$]-1-Li(L)$_n$-2,4-(SiMe$_3$)$_2$-2,4-$C_2B_4H_4$ (n = 2, L = THF; n = 1, L = TMEDA) with various magnesium reagents produced a number of different magnesacarboranes. The product of a 1:1 molar ratio reaction of the 2,3-C_2B_4 monosodium compound (R = SiMe$_3$ and L = TMEDA) with MeMgBr was the half-sandwich magnesacarborane *closo*-1-Mg(TMEDA)-2,3-(SiMe$_3$)$_2$-2,3-$C_2B_4H_4$ (**I**), while when R = Me, the same reaction conditions gave the novel full-exo-sandwich complex *commo-exo*-4,4′,5,5′-Mg(TMEDA)[2-(SiMe$_3$)-3-(Me)-2,3-$C_2B_4H_5$]$_2$ (**II**). The full-endo-sandwich magnesacarboranes [Na(THF)$_2$]$_2$[*commo*-1,1′-Mg{2,3-(SiMe$_3$)$_2$-2,3-$C_2B_4H_4$}$_2$] (**IV**) and [Na(TMEDA)]$_2$[*commo*-1,1′-Mg{2,3-(SiMe$_3$)$_2$-2,3-$C_2B_4H_4$}$_2$] (**V**) were the exclusive products when the appropriate monosodium compound reacted with Mg(Bu)$_2$ in 2:1 molar ratios. Reaction of *closo-exo*-5,6-[(μ-H)$_2$Li(TMEDA)]-1-Li(TMEDA)-2,4-(SiMe$_3$)$_2$-2,4-$C_2B_4H_4$ with MgBr$_2$ in a 1:1 molar ratio produced *closo*-1-Mg(TMEDA)-2,4-(SiMe$_3$)$_2$-2,4-$C_2B_4H_4$ (**III**), while a 2:1 molar ratio gave [Li(TMEDA)$_2$]$_2$[*commo*-1,1′-Mg{2,4-(SiMe$_3$)$_2$-2,4-$C_2B_4H_4$}$_2$] (**VI**). The yields ranged from 73% for **III** to 94% for **II**. On the other hand, the 1:1 molar ratio reaction of the THF-solvated 2,4-C_2B_4 disodium compound with MeMgBr, followed by the addition of 1 equiv of the THF-solvated monosodium compound of the 2,3-C_2B_4 carborane did not give the expected mixed-ligand complex but produced a 50:50 mixture of **IV** and [Li(THF)$_2$]$_2$[*commo*-1,1′-Mg{2,4-(SiMe$_3$)$_2$-2,4-$C_2B_4H_4$}$_2$] (**VII**) in nearly quantitative yields. The magnesacarboranes were characterized by their infrared spectra, chemical analysis, H^1, ^{11}B, and ^{13}C NMR spectra, and, in the case of **VII**, by its ^7Li NMR spectrum. Compounds **I**, **II**, and **IV** were further characterized by single-crystal X-ray analysis. Compound **I** crystallizes as a dimer in which a Mg occupies the apical position above the pentagonal face of one carborane and is bonded to the unique boron of the other carborane in the dimer through a Mg−H−B bridge. The structure of **II** is one in which a TMEDA-solvated Mg is exo-polyhedrally bonded to two 2,3-C_2B_4 monoanionic ligands through a pair of Mg−H−B bridges, while in **IV**, the two carborane dianions are η^5-bonded to a Mg in a more conventional endo-sandwich complex. The reactions with MeMgBr are thought to proceed through the formation of a methylmagnesacarborane intermediate which undergoes further reaction to give the final products. The ^{11}B NMR spectra of **I**−**VII** were analyzed with the aid of ab initio GIAO molecular orbital calculations.

Introduction

There have been a number of reports of the incorporation of metals, or metal groups, into the polyhedral cage structures of carboranes.[1] Although a variety of carboranes have been investigated, most cage expansion studies are those involving the dicarbaboranes having four or nine boron atoms, which result in the respective pentagonal bipyramidal (MC_2B_4) or icosahedral (MC_2B_9) metallacarboranes.[1] The most common method of synthesis is the reaction of the particular *nido*-carborane anion with a suitable metal halide reagent. The counterions of the precursor carborane ligands are usually one of the group 1 metals,[1,2] although aluminum,[3] thallium(I)[4,5] and tin(II)[6] counterions have also been

† Camille and Henry Dreyfus Scholar.

(1) (a) Grimes, R. N. In *Comprenensive Organometallic Chemistry II*; Abel, E. W., Stone, F. G. A., Wilkinson, G., Eds.; Elsevier Science: New York, 1995; Vol. 1, Chapter 9. (b) Saxena, A. K.; Maguire, J. A.; Hosmane, N. S. *Chem. Rev.* **1997**, *97*, 2421.

(2) (a) Hawthorne, M. F.; Young, D. C.; Wegner, P. A. *J. Am. Chem. Soc.* **1965**, *87*, 1818. (b) Hawthorne, M. F. *Acc. Chem. Res.* **1968**, *1*, 281.

(3) Jutzi, P.; Galow, P. *J. Organomet. Chem.*, **1987**, *319*, 139.

(4) Spencer, J. L.; Green, M.; Stone, F. G. A. *J. Chem. Soc., Chem. Commun.* **1972**, 1178.

S0276-7333(97)01113-8 CCC: $15.00
Publication on Web 03/04/1998

used. The group 1 metals have generally been assumed to be innocent spectators whose interactions have been ignored. However, structural studies on the bis(trimethylsilyl)-substituted C_2B_4 carborane derivatives have shown that the group 1 metals can occupy apical positions above the C_2B_3 pentagonal faces of the ligands to form stable half-sandwich complexes[7] and in the case of lithium, a full-sandwich complex.[8] It has also been demonstrated that the structures exert an influence on the reactivity of these compounds.[7a,9] It would be of great interest to compare the structures and reactivities of these metallacarboranes with those of the other *s*-block elements. Unfortunately, there is little information available on the group 2 metallacarboranes. The only structures of larger cage group 2 metallacarboranes are those of *closo*-1,1,1,1-(MeCN)$_4$-1,2,4-$CaC_2B_{10}H_{12}$[10] and [*closo*-1,1,1-(MeCN)$_3$-1,2,4-$SrC_2B_{10}H_{12}$]$_n$,[11] reported by Hawthorne and co-workers. The beryllacarborane, $Me_3NBeC_2B_9H_{11}$ was synthesized and assigned a closo structure on the basis of its NMR spectrum.[12] The only group 2 metallacarborane structures in the smaller, C_2B_4-cage system were those contained in our preliminary report on half- and full-sandwich magnesacarboranes that were synthesized by the reaction of *nido*-1-Na(L)$_2$-2,3-($SiMe_3$)$_2$-2,3-$C_2B_4H_5$ (L = TMEDA or THF) with magnesium alkyls.[13] We report herein the details of the synthetic, spectroscopic, and structural studies of these compounds, as well as the results of an extension of our investigation of the syntheses and structures of the group 2 metallacarboranes.

Experimental Section

Materials. 2,3-Bis(trimethylsilyl)-2,3-dicarba-*nido*-hexaborane(8), 2-(trimethylsilyl)-3-(methyl)-2,3-dicarba-*nido*-hexaborane(8), and 1,2-bis(trimethylsilyl)-1,2-dicarba-*closo*-hexaborane-(6) were prepared using the literature methods.[7b,14,15] The *closo*-carborane was subsequently converted to the corresponding *N*,*N*,*N*,*N*-tetramethylethylenediamine (TMEDA)- or tetrahydrofuran (THF)-solvated carbons-apart dilithiacarborane *closo-exo*-5,6-[(μ-H)$_2$Li(L)$_n$]-1-Li(L)$_n$-2,4-($SiMe_3$)$_2$-2,4-$C_2B_4H_4$ (L = TMEDA, n = 1; L = THF, n = 2) by reduction with Li/$C_{10}H_8$ as outlined previously.[16] The *nido*-carborane precursor was converted to the corresponding THF- or TMEDA-solvated monosodium compound *nido*-1-Na(L)-2-($SiMe_3$)-3-(R)-2,3-$C_2B_4H_5$ (L = TMEDA or THF; R = $SiMe_3$, Me), as previously described.[7b] Prior to use, TMEDA (Aldrich) was distilled in vacuo and stored over sodium metal; its purity was checked by IR and NMR spectra and boiling point measurements. Before use, naphthalene (Aldrich) was sublimed in vacuo and Li metal (Aldrich) was freshly cut in a drybox. $MgBr_2$ was freshly prepared by the reaction of magnesium with 1,2-dibromoethane in anhydrous THF at room temperature. MeMgBr (3.0 M solution in diethyl ether; Aldrich) and Mg(n-C_4H_9)$_2$ (1.0 M solution in heptane; Aldrich) were used as received. Benzene, THF, and *n*-hexane were dried over $LiAlH_4$ and doubly distilled; all other solvents, including C_6D_6 and THF-d_8 (Aldrich), were dried over 4−8 mesh molecular sieves (Aldrich) and either saturated with dry argon or degassed before use.

Spectroscopic and Analytical Procedures. ^{1}H, ^{7}Li, ^{11}B, and ^{13}C pulse Fourier transform NMR spectra at 200, 77.7, 64.2, and 50.3 MHz, respectively, were recorded on an IBM-WP200 SY multinuclear NMR spectrometer. Infrared spectra were recorded on a Nicolet Magna 550 FT-IR spectrophotometer. Elemental analyses were obtained from E+R Microanalytical Laboratory, Inc., Corona, NY.

Synthetic Procedures. All experiments were carried out in Pyrex round-bottom flasks of 100−250 mL capacities, containing magnetic stirring bars and fitted with high-vacuum Teflon valves. Nonvolatile substances were manipulated in either a drybox or an evacuable glovebag under an atmosphere of dry nitrogen. All known compounds among the products were identified by comparing their IR and NMR spectra with those of authentic samples.

Synthesis of *closo*-1-Mg(TMEDA)-2,3-($SiMe_3$)$_2$-2,3-$C_2B_4H_4$ (I). To a solution of MeMgBr (3.0 mmol) in 1 mL of Et_2O, a benzene solution (20 mL) of *nido*-1-Na(TMEDA)-2,3-($SiMe_3$)$_2$-2,3-$C_2B_4H_5$ (1.07 g, 3.0 mmol) was added at −78 °C. The mixture was warmed to room temperature, which resulted in the slow evolution of gas with the concomitant formation of a white solid. After the mixture was stirred constantly overnight at room temperature, it was filtered in vacuo to collect a clear filtrate. The white solid that remained on the frit was identified as NaBr (not measured) and was discarded. Removal of the solvent from the filtrate resulted in the formation of a pale yellow solid, which was washed repeatedly with *n*-hexane and later identified as *closo*-1-Mg(TMEDA)-2,3-($SiMe_3$)$_2$-2,3-$C_2B_4H_4$ (**I**) (0.94 g, 2.60 mmol, 87% yield; mp 290 °C; soluble in both polar and nonpolar organic solvents). Compound **I** was recrystallized from benzene solution to give colorless platelike crystals. Anal. Calcd for $C_{14}H_{38}B_4N_2Si_2Mg$ (**I**): C, 46.95; H, 10.69; N, 7.81. Found: C, 47.89; H, 10.37; N, 7.03. The NMR and IR spectral data of **I** are listed in Tables 1 and 2, respectively.

Synthesis of *commo-exo*-4,4′,5,5′-Mg(TMEDA)[2-($SiMe_3$)-3-(Me)-2,3-$C_2B_4H_5$]$_2$(II). To a solution of MeMgBr (3.0 mmol) in 1 mL Et_2O, a benzene solution of (20 mL) of *nido*-1-Na-(TMEDA)-2-($SiMe_3$)-3-(Me)-2,3-$C_2B_4H_5$ (0.90 g, 3.0 mmol) was added at −78 °C. The mixture was warmed to room temperature, which resulted in the formation of a white precipitate, but no gas evolution was detected. After the mixture was stirred constantly overnight at room temperature, it was filtered in vacuo to collect a clear filtrate. Removal of solvents

(5) (a) Schubert, D. M.; Bandman, M. A.; Rees, W. S., Jr.; Knobler, C. B.; Lu, P.; Nam, W.; Hawthorne, M. F. *Organometallics* **1990**, *9*, 2046. (b) Bandman, M. A.; Knobler, C. B.; Hawthorne, M. F. *Inorg. Chem.* **1989**, *28*, 8, 1204. (c) Maning, M. J.; Knobler, C. B.; Hawthorne, M. F. *J. Am. Chem. Soc.* **1988**, *110*, 4458.

(6) (a) Islam, M. S.; Siriwardane, U.; Hosmane, N. S.; Maguire, J. A.; de Meester, P.; Chu, S. S. C. *Organometallics* **1987**, *6*, 1936. (b) Siriwardane, U.; Islam, M. S.; Maguire, J. A.; Hosmane, N. S. *Organometallics* **1988**, *7*, 1893.

(7) (a) Hosmane, N. S.; Siriwardane, U.; Zhang, G.; Zhu, H.; Maguire, J. A. *J. Chem. Soc., Chem. Commun.* **1989**, 1128. (b) Hosmane, N. S.; Saxena, A. K.; Barreto, R. D.; Zhang, H.; Maguire, J. A.; Jia, L.; Wang, Y.; Oki, A. R.; Grover, K. V.; Whitten, S. J.; Dawson, K.; Tolle, M. A.; Siriwardane, U.; Demissie, T.; Fagner, J. S. *Organometallics* **1993**, *12*, 2, 3001. (c) Zhang, H.; Wang, Y.; Saxena, A. K.; Oki, A. R.; Maguire, J. A.; Hosmane, N. S. *Organometallics* **1993**, *12*, 3933.

(8) Hosmane, N. S.; Yang, J.; Zhang, H.; Maguire, J. A. *J. Am. Chem. Soc.* **1996**, *118*, 5150.

(9) (a) Hosmane, N. S.; Jia, L.; Wang, Y.; Saxena, A. K.; Zhang, H.; Maguire, J. A. *Organometallics* **1994**, *13*, 4113. (b) Wang, Y.; Zhang, H.; Maguire, J. A.; Hosmane, N. S. *Organometallics* **1993**, *12*, 3781.

(10) Khattar, R.; Knobler, C. B.; Hawthorne, M. F. *J. Am. Chem. Soc.* **1990**, *112*, 4962.

(11) Khattar, R.; Knobler, C. B.; Hawthorne, M. F. *Inorg. Chem.* **1990**, *29*, 2191.

(12) (a) Popp, G.; Hawthorne, M. F. *J. Am. Chem. Soc.* **1968**, *90*, 6553. (b) Popp, G.; Hawthorne, M. F. *Inorg. Chem.* **1971**, *10*, 391.

(13) Hosmane, N. S.; Zhu, D.; McDonald, J. E.; Zhang, H.; Maguire, J. A.; Gray, T. G.; Helfert, S. C. *J. Am. Chem. Soc.* **1995**, *117*, 12362.

(14) (a) Hosmane, N. S.; Sirmokadam, N. N.; Mollenhauer, M. N. *J. Organomet. Chem.* **1985**, *279*, 359. (b) Hosmane, N. S.; Mollenhauer, M. N.; Cowley, A. H.; Norman, N. C. *Organometallics* **1985**, *4*, 1194. (c) Barreto, R. D.; Hosmane, N. S. *Inorg. Synth.* **1992**, *29*, 89.

(15) Hosmane, N. S.; Barreto, R. D.; Tolle, M. A.; Alexander, J. J.; Quintana, W.; Siriwardane, U.; Shore, S. G.; Williams, R. E. *Inorg. Chem.* **1990**, *29*, 2698.

(16) (a) Hosmane, N. S.; Jia, L.; Zhang, H.; Bausch, J. W.; Prakash, G. K. S.; Williams, R. E.; Onak, T. P. *Inorg. Chem.* **1991**, *30*, 3793. (b) Jia, L. M.S. Thesis, Southern Methodist University, Dallas, Texas, 1992. (c) Zhang, H.; Wang, Y.; Saxena, A. K.; Oki, A. R.; Maguire, J. A.; Hosmane, N. S. *Organometallics* **1993**, *12*, 3933.

Table 1. NMR Spectral Data of Magnesacarboranes I–VII[a]

	^{11}B NMR (64.21 MHz, external $BF_3{\cdot}OEt_2$)
I	18.58 (br, 2B, basal BH, $^1J(^{11}B-^1H)$ = unresolved), −0.28 (br, 1B, basal BH, $^1J(^{11}B-^1H)$ = unresolved), −49.77 (d, 1B, apical BH, $^1J(^{11}B-^1H)$ = 144.5 Hz)
II	4.50 (br, 2B, basal BH, $^1J(^{11}B-^1H)$ = unresolved), −5.70 (br, 1B, basal BH, $^1J(^{11}B-^1H)$ = unresolved), −50.11 (d, 1B, apical BH, $^1J(^{11}B-^1H)$ = 158.2 Hz)
III	16.0 (br, 1B, basal BH, $^1J(^{11}B-^1H)$ = unresolved), 7.96 (br, 2B, basal BH, $^1J(^{11}B-^1H)$ = unresolved), −49.74 (d, 1B, apical BH, $^1J(^{11}B-^1H)$ = 161.2 Hz)
IV[b]	21.28 (br, 1B, basal BH, $^1J(^{11}B-^1H)$ = unresolved), 17.88 (br, 1B, basal BH, $^1J(^{11}B-^1H)$ = unresolved), 6.74 (br, 1B, basal BH, $^1J(^{11}B-^1H)$ = unresolved), −48.34 (br, 1B, apical BH, $^1J(^{11}B-^1H)$ = 121.1 Hz)
V[b]	16.66 (br, 2B, basal BH, $^1J(^{11}B-^1H)$ = unresolved), 1.30 (br, 1B, basal BH, $^1J(^{11}B-^1H)$ = unresolved), −53.73 (d, 1B, apical BH, $^1J(^{11}B-^1H)$ = 139 Hz)
VI	16.70 (br, 1B, basal BH, $^1J(^{11}B-^1H)$ = unresolved), 4.16 (br, 2B, basal BH, $^1J(^{11}B-^1H)$ = unresolved), −55.46 (d, 1B, apical BH, $^1J(^{11}B-^1H)$ = 160.2 Hz)
VII	16.00 (br, 1B, basal BH, $^1J(^{11}B-^1H)$ = unresolved), 4.52 (br, 2B, basal BH, $^1J(^{11}B-^1H)$ = unresolved), −54.76 (d, 1B, apical BH, $^1J(^{11}B-^1H)$ = 152.4 Hz)
	^{1}H NMR (200.13 MHz, external Me_4Si)
I	2.19 (s, 12H, Me, TMEDA), 1.67 (s, 4H, CH_2, TMEDA), 0.65 (s, 18H, $SiMe_3$)
II	2.49 (s, 6H, Me), 1.86 (s, 12H, Me, TMEDA), 1.60 (s, 4H, CH_2, TMEDA), 0.51 (s, 18H, $SiMe_3$), −3.9 (vbr, bridge H)
III	2.16 (s, 12H, Me, TMEDA), 1.85 (s, 4H, CH_2, TMEDA), 0.39 (s, 18H, $SiMe_3$)
IV[b]	3.62 (m, 16H, CH_2, THF), 1.77 (m, 16H, CH_2, THF), 0.20 (s, 36H, $SiMe_3$)
V	2.20 (s, 24H, Me, TMEDA), 2.03 (s, 8H, CH_2, TMEDA), 0.70 (s, 36H, $SiMe_3$)
VI	2.13 (s, 48H, Me, TMEDA), 1.79 (s, 16H, CH_2, TMEDA), 0.59 (s, 36H, $SiMe_3$)
VII	3.64 (m, 16 H, CH_2, THF), 1.48 (m, 16H, CH_2, THF), 0.62 (s, 36H, $SiMe_3$)
	^{13}C NMR (50.32 MHz, external Me_4Si)
I	101.33 (s(br), cage carbons (SiCB)), 56.00 (t, CH_2, TMEDA, $^1J(^{13}C-^1H)$ = 137.0 Hz), 47.89 (q, CH_3, TMEDA, $^1J(^{13}C-^1H)$ = 137.5 Hz), 4.13 (q, $SiMe_3$, $^1J(^{13}C-^1H)$ = 116 Hz)
II	135.26 (s(br), cage carbon, (SiCB)), 112.03 (s(br), cage carbon, (BCMe)), 55.86 (t, CH_2, TMEDA, $^1J(^{13}C-^1H)$ = 137.5 Hz), 47.02 (q, CH_3, TMEDA, $^1J(^{13}C-^1H)$ = 135.4 Hz), 23.50 (q, Me, $^1J(^{13}C-^1H)$ = 124.6 Hz), 1.56 (q, $SiMe_3$, $^1J(^{13}C-^1H)$ = 118.2 Hz)
III	87.97 (s(br), cage carbons (SiCB)), 56.08 (t, CH_2, TMEDA, $^1J(^{13}C-^1H)$ = 135.4 Hz), 46.69 (q, CH_3, TMEDA, $^1J(^{13}C-^1H)$ = 135.4 Hz), 2.17 (q, $SiMe_3$, $^1J(^{13}C-^1H)$ = 118.2 Hz)
IV[b]	103.20 (s(br), cage carbons (SiCB)), 68.24 (t, CH_2, THF, $^1J(^{13}C-^1H)$ = 145.0 Hz), 26.37 (t, CH_2, THF, $^1J(^{13}C-^1H)$ = 132.1 Hz), 3.91 (q, $SiMe_3$, $^1J(^{13}C-^1H)$ = 118.2 Hz)
V[b]	102.57 (s(br), cage carbons (SiCB)), 57.96 (t, CH_2, TMEDA, $^1J(^{13}C-^1H)$ = 133.2 Hz), 45.62 (q, CH_3, TMEDA, $^1J(^{13}C-^1H)$ = 133.2 Hz), 3.28 (q, $SiMe_3$, $^1J(^{13}C-^1H)$ = 118.2 Hz)
VI	93.21 (s(br), cage carbons (SiCB)), 56.37 (t, CH_2, TMEDA, $^1J(^{13}C-^1H)$ = 133.2 Hz), 46.21 (q, CH_3, TMEDA, $^1J(^{13}C-^1H)$ = 135.4 Hz), 2.37 (q, $SiMe_3$, $^1J(^{13}C-^1H)$ = 118.2 Hz)
VII	93.30 (s(br), cage carbons (SiCB)), 68.88 (t, CH_2, THF, $^1J(^{13}C-^1H)$ = 148.24 Hz), 25.42 (t, CH_2, THF, $^1J(^{13}C-^1H)$ = 133.2 Hz), 2.41 (q, $SiMe_3$, $^1J(^{13}C-^1H)$ = 116.02 Hz)
	^{7}Li NMR (77.7 MHz, external $LiNO_3$)
VII	1.17 (s, br)

[a] C_6D_6 was used as the solvent except where indicated. [b] THF-d_8 was used as the solvent.

Table 2. IR Spectral Data of Magnesacarboranes I–VII[a]

I	3050.3 (w), 2950.7 (s), 2900.8 (s), 2851.0 (s), 2807.4 (m) [(CH)], 2533.2 (s), 2470.9 (s) [(BH)], 1474.0 (s), 1299.6 (m), 1243.5 (s), 1168.7 (m), 1131.3 (m), 1031.6 (m), 950.6 (m), 838.5 (vs), 763.7 (m), 695.2 (m), 640.0 (m)
II	2958.8 (s), 2922.2 (s), 2859.4 (s) [(CH)], 2561.3 (s), 2503.7 (s), 2446.2 (s) [(BH)], 1912.7 (m), 1865.6 (m) [(B−H−B), bridge], 1447.6 (s), 1332.0 (s), 1253.6 (s), 1175.1 (m), 1107.1 (m), 877.0 (s), 840.3 (s), 819.4 (s), 756 (m)
III	2967.3 (s), 2891.6 (s), 2795.2 (s) [(CH)], 2547.4 (s), 2492.4 (s), 2451.1 (s) [(BH)], 1460.1 (s), 1363.7 (s), 1301.8 (s), 1239.8 (s), 1177.9 (m), 1129.7 (m), 1074.7 (s), 957.7 (s), 847.5 (vs), 799.4 (s), 634.2 (m), 592.9 (m)
IV[b]	2795.5 (m) [(CH)], 2522.6 (m), 2484.3 (s), 2433.4 (s), 2393.8 (m) [(BH)], 1466.0 (m), 1245.3 (s), 1188.7 (s), 1137.8 (m), 838.0 (vs), 758.8 (s), 685.2 (s), 634.3 (s)
V[b]	2762.3 (s) [(CH)], 2481.0 (s) 2439.3 (s), 2397.6 (s) [(BH)], 1465.2 (s), 1251.7 (s), 1184.0 (s), 996.5 (m), 840.2 (vs), 762.1 (s), 683.9 (s), 637.0 (s)
VI	2963.6 (s), 2876.9 (s), 2836.8 (s), 2790.2 (s) [(CH)], 2623.4 (s), 2583.4 (s), 2563.3 (s) [(BH)], 1456.0 (s), 1362.6 (m), 1295.9 (s), 1255.8 (s), 1162.4 (m), 1069.0 (m), 955.6 (s), 848.9 (s), 795.5 (s), 588.7 (m), 555.4 (m)
VII	2955.5 (s), 2888.9 (s) [(CH)], 2532.0 (s), 2495.7 (s), 2405.0 (s) [(BH)], 1461.2 (m), 1406.8 (m), 1370.5 (m), 1303.9 (m), 1243.4 (s), 1189.0 (s), 1049.8 (s), 947.0 (m), 886.5 (s), 844.1 (vs), 765.5 (s), 686.8 (s), 632.4 (s)

[a] C_6H_6 vs C_6H_6 except where indicated. Legend: v = very, s = strong or sharp, m = medium, w = weak, sh = shoulder, and br = broad. [b] THF vs THF.

from the filtrate resulted in the formation of a pale yellow solid, which was recrystallized from a benzene solution as colorless crystals and later identified as *commo-exo*-4,4′,5,5′-Mg(TMEDA)[2-($SiMe_3$)-3-(Me)-2,3-$C_2B_4H_5$]$_2$ (**II**) (0.65 g, 1.40 mmol, 94% yield; mp > 300 °C; soluble in both polar and nonpolar organic solvents). Anal. Calcd for $C_{18}H_{50}B_8N_2Si_2Mg$ (**II**): C, 46.84; H, 10.92; N, 6.07. Found: C, 47.85; H, 10.94; N, 6.36. The NMR and IR spectral data of **II** are listed in Tables 1 and 2, respectively.

Synthesis of *closo*-1-Mg(TMEDA)-2,4-($SiMe_3$)$_2$-2,4-$C_2B_4H_4$ (III). A 2.51 g (5.44 mmol) amount of *closo-exo*-5,6-[(μ-H)$_2$Li(TMEDA)]-1-Li(TMEDA)-2,4-($SiMe_3$)$_2$-2,4-$C_2B_4H_4$ was reacted with 1.0 g (5.44 mmol) of $MgBr_2$ in 30 mL of benzene at room temperature with constant stirring for 24 h. The reaction mixture was then filtered to collect a pale yellow filtrate. The white solid on the frit, identified as LiBr (not measured), was discarded. Removal of the solvent from the filtrate resulted in the formation of an off-white solid, which was washed with *n*-hexane and later identified as *closo*-1-Mg(TMEDA)-2,4-($SiMe_3$)$_2$-2,4-$C_2B_4H_4$ (**III**) (1.43 g, 3.99 mmol, 73% yield; mp > 250 °C (dec); soluble in both polar and nonpolar organic solvents). Compound **III** was recrystallized from its benzene solution to yield colorless crystals. Anal. Calcd for $C_{14}H_{38}B_4N_2Si_2Mg$ (**III**): C, 46.95; H, 10.69; N, 7.81. Found: C, 47.12; H, 10.63; N, 8.01. The NMR and IR spectral data of **III** are listed in Tables 1 and 2, respectively.

Table 3. Crystallographic Data[a] for Magnesacarboranes I, II, and IV

	I	II	IV
formula	$C_{34}H_{82}N_4B_8Si_4Mg_2$	$C_{18}H_{50}N_2B_8Si_2Mg$	$C_{32}H_{76}B_8O_4Na_2Si_4Mg$
fw	794.5	461.6	794.1
space group	$P\bar{1}$	$C2/c$	$C2/c$
a, Å	13.609(2)	12.403(5)	21.997(6)
b, Å	14.391(2)	18.807(7)	13.417(4)
c, Å	15.021(2)	13.496(5)	17.386(5)
α, deg	89.440(10)	90	90
β, deg	63.490(10)	95.16(3)	91.28(2)
γ, deg	81.280(10)	90	90
V, Å^3	2596.4(7)	3136(2)	5137(4)
Z	2	4	4
D_{calcd}, g cm^{-3}	1.016	0.978	1.027
abs coeff, mm^{-1}	0.165	0.142	0.174
cryst dimens, mm	0.40 × 0.30 × 0.15	0.25 × 0.35 × 0.20	0.10 × 0.35 × 0.30
scan type	$\omega/2\theta$	$\omega/2\theta$	$\omega/2\theta$
scan speed in ω; min, max	5.33, 29.30	5.33, 29.30	5.33, 29.30
2θ range, deg	3.0−42.0	3.0−44.0	3.0−42.0
T, K	220	228	230
decay, %	0	0	0
no. of data collected	5872	1113	2862
no. of obsd reflctns, $F>6.0\sigma(F)$	4419	1113	1139
no. of params refined	494	141	202
GOF	1.50	1.59	2.50
$\Delta\rho_{(max, min)}$, e/Å^3	0.32, −0.23	0.38, −0.25	0.62, −0.36
R^b	0.0387	0.0585	0.0948
w$R^{c,d}$	0.0574	0.0751	0.1193

[a] Graphite-monochromated Mo Kα radiation, $\lambda = 0.710\ 73$ Å. [b] $R = \sum||F_o| - |F_c||/\sum|F_o|$, w$R = [\sum w(F_o - F_c)^2/\sum w(F_o)^2]^{1/2}$. [c] $w = 1/[\sigma^2(F_o) + 0.001(F_o)^2]$. [d] $w = 1/[\sigma^2(F_o^2) + (0.0410P)^2 + 14.4051P]$, where $P = (F_o^2 + 2F_c^2)/3$.

Synthesis of [Na(THF)$_2$]$_2$[*commo*-1,1′-Mg{2,3-(SiMe$_3$)$_2$-2,3-C$_2$B$_4$H$_4$}$_2$] (IV). To a solution of (n-C$_4$H$_9$)$_2$Mg (3.2 mmol) in 3.2 mL of heptane, a benzene solution (25 mL) of *nido*-1-Na(THF)$_2$-2,3-(SiMe$_3$)$_2$-2,3-C$_2$B$_4$H$_5$ (2.03 g, 6.45 mmol) was slowly added in vacuo at 0 °C. The mixture was then warmed to room temperature and stirred overnight, during which time slow evolution of a gas and the concomitant formation of a white precipitate were observed. All of the solvents were then removed from the mixture to give a pale yellow solid, which was washed with anhydrous benzene to yield [Na(THF)$_2$]$_2$-[*commo*-1,1′-Mg{2,3-(SiMe$_3$)$_2$-2,3-C$_2$B$_4$H$_4$}$_2$] (**IV**) as a white solid (2.08 g, 2.64 mmol, 82% yield; mp 320 °C(dec); soluble in THF and slightly soluble in nonpolar solvents such as benzene). Compound **IV** was recrystallized from a THF solution to give colorless crystals. Anal. Calcd for C$_{32}$H$_{76}$B$_8$O$_4$Si$_4$Na$_2$-Mg (**IV**): C, 48.48; H, 9.59. Found: C, 48.28; H, 9.50. The NMR and IR spectral data of **IV** are listed in Tables 1 and 2, respectively.

Synthesis of [Na(TMEDA)]$_2$[*commo*-1,1′-Mg{2,3-(SiMe$_3$)$_2$-2,3-C$_2$B$_4$H$_4$}$_2$] (V). In a procedure identical to that described above for **IV**, the reaction between 3.2 mmol of (n-C$_4$H$_9$)$_2$Mg in pentane and 6.77 mmol (2.42 g) of the TMEDA-solvated monosodium compound gave a white solid, identified as [Na-(TMEDA)]$_2$[*commo*-1,1′-Mg{2,3-(SiMe$_3$)$_2$-2,3-C$_2$B$_4$H$_4$}$_2$] (**V**), in 84% yield (2.09 g, 2.84 mmol; mp >250 °C; soluble in polar organic solvents and slightly soluble in nonpolar organic solvents). Compound **V** was later recrystallized from a THF solution to give colorless crystals. Anal. Calcd for C$_{28}$H$_{76}$B$_8$N$_4$-Si$_4$Na$_2$Mg (**V**): C, 47.64; H, 10.85; N, 7.93. Found: C, 47.94; H, 10.79; N, 8.03. The NMR and IR spectral data of **V** are listed in Tables 1 and 2, respectively.

Synthesis of [Li(TMEDA)$_2$]$_2$[*commo*-1,1′-Mg{2,4-(SiMe$_3$)$_2$-2,4-C$_2$B$_4$H$_4$}$_2$] (VI). To a suspension of MgBr$_2$ (0.40 g, 2.17 mmol) in 10 mL of benzene, a solution of 2.02 g (4.36 mmol) of *closo-exo*-5,6-[(μ-H)$_2$Li(TMEDA)]-1-Li(TMEDA)-2,4-(SiMe$_3$)$_2$-2,4-C$_2$B$_4$H$_4$ in 20 mL of benzene was added at 0 °C. The resulting mixture was warmed to room temperature and stirred overnight, during which time a white precipitate formed. The mixture was filtered in vacuo to collect the pale yellow filtrate. The white solid on the frit, identified as LiBr (not measured), was discarded. Removal of the solvent from the filtrate gave an off-white solid, which was washed with n-hexane to collect a white solid. This solid was later identified as [Li(TMEDA)$_2$]$_2$[*commo*-1,1′-Mg{2,4-(SiMe$_3$)$_2$-2,4-C$_2$B$_4$H$_4$}$_2$] (**VI**) (1.74 g, 1.86 mmol, 85% yield; mp > 250 °C; soluble in polar solvents and partially soluble in nonpolar solvents). Compound **VI** was recrystallized from a benzene solution to give colorless crystals. Anal. Calcd for C$_{40}$H$_{108}$B$_8$N$_8$Si$_4$Li$_2$Mg (**VI**): C, 51.20; H, 11.52. Found: C, 52.94; H, 10.69. The NMR and IR spectral data of **VI** are listed in Tables 1 and 2, respectively.

Attempted Synthesis of the Mixed-Ligand Magnesacarborane Sandwich [LiNa(THF)$_4$]-[*commo*-1,1′-Mg{2,4-(SiMe$_3$)$_2$-2,4-C$_2$B$_4$H$_4$}{2,3-(SiMe$_3$)$_2$-2,3-C$_2$B$_4$H$_4$}], and the Synthesis of [Li(THF)$_2$]$_2$[*commo*-1,1′-Mg{2,4-(SiMe$_3$)$_2$-2,4-C$_2$B$_4$H$_4$}$_2$] (VII). A solution of 4.46 mmol of *closo-exo*-5,6-[(μ-H)$_2$Li(THF)$_2$]-1-Li(THF)$_2$-2,4-(SiMe$_3$)$_2$-2,4-C$_2$B$_4$H$_4$ in 25 mL of benzene was added to a solution of 4.46 mmol of CH$_3$MgBr in diethyl ether at −78 °C, and the mixture was then warmed to room temperature and stirred for 4 h. To the resulting mixture, a solution of 1.59 g (4.46 mmol) of *nido*-1-Na(THF)-2,3-(SiMe$_3$)$_2$-2,3-C$_2$B$_4$H$_5$ was added at 0 °C, and the mixture was then stirred overnight. Filtration of the reaction mixture gave a brown solution, from which all solvents were removed to generate a yellow solid. The solid was washed with n-hexane and was then partially dissolved in 15 mL of benzene. The resulting mixture was filtered in vacuo to give a white solid and a brown solution. The white solid was later spectroscopically identified as [Na(THF)$_2$]$_2$[*commo*-1,1′-Mg{2,3-(SiMe$_3$)$_2$-2,3-C$_2$B$_4$H$_4$}$_2$] (**IV**) (1.39 g, 1.76 mmol, 79% yield). From the brown solution, colorless crystals were obtained and later identified as [Li(THF)$_2$]$_2$[*commo*-1,1′-Mg{2,4-(SiMe$_3$)$_2$-2,4-C$_2$B$_4$H$_4$}$_2$] (**VII**) (1.50 g, 1.97 mmol, 88%; mp > 250 °C; soluble in both polar and nonpolar organic solvents). Anal. Calcd for C$_{32}$H$_{76}$B$_8$O$_4$Si$_4$Li$_2$Mg (**VII**): C, 50.42; H, 10.05. Found: C, 49.75; H, 10.26. The NMR and IR spectral data of **VII** are listed in Tables 1 and 2, respectively.

Crystal Structure Analysis of *closo*-1-Mg(TMEDA)-2,3-(SiMe$_3$)$_2$-2,3-C$_2$B$_4$H$_4$ (I), *commo-exo*-4,4′,5,5′-Mg(TMEDA)$_2$-[2-(SiMe$_3$)-3-(Me)-2,3-C$_2$B$_4$H$_5$]$_2$ (II), and [Na(THF)$_2$]$_2$-[*commo*-1,1′-Mg{2,3-(SiMe$_3$)$_2$-2,3-C$_2$B$_4$H$_4$}$_2$] (IV). Colorless, transparent, X-ray quality crystals of the magnesacarboranes **I**, **II**, and **IV** were grown very slowly from their respective benzene and THF solutions. The crystals were transferred to

Table 4. Selected Bond Lengths (Å) and Bond Angles (deg) for Magnesacarboranes I, II, and IV

Bond Lengths (Å)

Compound **I**

Mg(1)−Mg(2)	3.426 (2)	Mg(2)−B(24)	2.404 (3)	B(15)−B(16)	1.781 (4)
Mg(1)−C(11)	2.649 (3)	Mg(2)−B(25)	2.471 (3)	C(21)−C(22)	1.507 (4)
Mg(1)−C(12)	2.635 (3)	Mg(2)−N(61)	2.325 (3)	C(21)−B(25)	1.573 (5)
Mg(1)−B(13)	2.493 (3)	Mg(2)−N(62)	2.256 (2)	C(21)−B(26)	1.692 (4)
Mg(1)−B(14)	2.393 (3)	C(11)−C(12)	1.521 (4)	C(22)−B(23)	1.564 (5)
Mg(1)−B(15)	2.472 (4)	C(11)−B(15)	1.565 (5)	C(22)−B(26)	1.708 (3)
Mg(1)−B(24)	2.540 (5)	C(11)−B(16)	1.699 (4)	B(23)−B(24)	1.661 (4)
Mg(1)−N(51)	2.327 (2)	C(12)−B(13)	1.566 (6)	B(23)−B(26)	1.782 (5)
Mg(1)−N(52)	2.252 (2)	C(12)−B(16)	1.714 (4)	B(24)−B(25)	1.635 (6)
Mg(2)−B(14)	2.534 (5)	B(13)−B(14)	1.645 (5)	B(24)−B(26)	1.761 (6)
Mg(2)−C(21)	2.621 (4)	B(13)−B(16)	1.786 (6)	B(25)−B(26)	1.771 (5)
Mg(2)−C(22)	2.596 (3)	B(14)−B(15)	1.648 (6)		
Mg(2)−B(23)	2.485 (3)	B(14)−B(16)	1.778 (6)		

Compound **II**

Mg−B(13)	2.383 (8)	C(11)−B(15)	1.525 (9)	B(14)−B(15)	1.767 (10)
Mg−B(14)	2.480 (7)	C(11)−B(16)	1.723 (9)	B(14)−B(16)	1.740 (10)
Mg−N(25)	2.183 (5)	C(12)−B(13)	1.502 (9)	B(15)−B(16)	1.762 (10)
Mg−B(13A)	2.383 (8)	C(12)−B(16)	1.753 (9)	N(25)−C(26)	1.476 (7)
Mg−B(14A)	2.480 (7)	C(12)−C(24)	1.515 (8)	N(25)−C(27)	1.491 (8)
Mg−N(25A)	2.183 (5)	B(13)−B(14)	1.663 (10)	N(25)−C(28)	1.475 (8)
C(11)−C(12)	1.458 (8)	B(13)−B(16)	1.787 (10)	C(26)−C(26A)	1.600 (11)

Compound **IV**

Mg−C(11)	2.446 (13)	Na−B(14)	2.867 (17)	C(12)−B(13)	1.552 (22)
Mg−C(12)	2.461 (14)	Na−B(16)	3.055 (18)	C(11)−B(16)	1.723 (22)
Mg−B(13)	2.420 (16)	Na−O(31)	2.234 (23)	C(12)−B(16)	1.676 (23)
Mg−B(14)	2.398 (16)	Na−O(32)	2.409 (24)	B(13)−B(14)	1.694 (25)
Mg−B(15)	2.405 (18)	Na−O(41)	2.308 (14)	B(13)−B(16)	1.749 (25)
Mg−C(11A)	2.446 (13)	Na−C(42)	3.117 (30)	B(14)−B(15)	1.593 (24)
Mg−C(12A)	2.461 (14)	Na−Na(A)	3.801 (11)	B(14)−B(16)	1.779 (24)
Mg−B(13A)	2.420 (16)	Na−B(14A)	2.883 (19)	B(14)−Na(A)	2.883 (19)
Mg−B(14B)	2.398 (16)	Na−B(15A)	2.831 (19)	B(15)−B(16)	1.776 (26)
Mg−B(15B)	2.405 (18)	C(11)−C(12)	1.509 (21)	B(15)−Na(A)	2.831 (19)
Na−B(13)	2.976 (17)	C(11)−B(15)	1.572 (23)		

Bond Angles (deg)

Compound **I**

Mg(2)−Mg(1)−C(11)	107.5(1)	C(11)−Mg(1)−B(15)	35.4(1)
Mg(2)−Mg(1)−C(12)	93.8(1)	C(12)−Mg(1)−B(15)	59.5(1)
C(11)−Mg(1)−C(12)	33.5(1)	B(13)−Mg(1)−B(15)	64.1(1)
Mg(2)−Mg(1)−B(13)	58.6(1)	B(14)−Mg(1)−B(15)	39.6(1)
C(11)−Mg(1)−B(13)	59.3(1)	Mg(2)−Mg(1)−B(24)	44.5(1)
C(12)−Mg(1)−B(13)	35.4(1)	C(11)−Mg(1)−B(24)	152.0(1)
Mg(2)−Mg(1)−B(14)	47.7(1)	C(12)−Mg(1)−B(24)	129.3(1)
C(11)−Mg(1)−B(14)	61.0(1)	B(13)−Mg(1)−B(24)	96.2(1)
C(12)−Mg(1)−B(14)	61.1(1)	B(14)−Mg(1)−B(24)	91.6(1)
B(13)−Mg(1)−B(14)	39.3(1)	B(15)−Mg(1)−B(24)	124.6(1)
Mg(2)−Mg(1)−B(15)	85.1(1)	Mg(2)−Mg(1)−N(51)	119.2(1)
C(11)−Mg(1)−N(51)	99.5(1)	C(22)−Mg(2)−B(24)	61.4(1)
C(12)−Mg(1)−N(51)	131.6(1)	B(23)−Mg(2)−B(24)	39.7(1)
B(13)−Mg(1)−N(51)	151.3(1)	Mg(1)−Mg(2)−B(25)	85.3(1)
B(14)−Mg(1)−N(51)	115.3(1)	B(14)−Mg(2)−B(25)	125.3(1)
B(15)−Mg(1)−N(51)	87.4(1)	C(21)−Mg(2)−B(25)	35.8(1)
B(24)−Mg(1)−N(51)	97.9(1)	C(22)−Mg(2)−B(25)	59.9(1)
Mg(2)−Mg(1)−N(52)	137.6(1)	B(23)−Mg(2)−B(25)	64.4(1)
C(11)−Mg(1)−N(52)	105.6(1)	B(24)−Mg(2)−B(25)	39.2(1)
C(12)−Mg(1)−N(52)	99.5(1)	Mg(1)−Mg(2)−N(61)	119.1(1)
B(13)−Mg(1)−N(52)	122.2(1)	B(14)−Mg(2)−N(61)	98.9(1)
B(14)−Mg(1)−N(52)	160.2(1)	C(21)−Mg(2)−N(61)	100.7(1)
B(15)−Mg(1)−N(52)	136.0(1)	C(22)−Mg(2)−N(61)	133.3(1)
B(24)−Mg(1)−N(52)	98.9(1)	B(23)−Mg(2)−N(61)	151.4(1)
N(51)−Mg(1)−N(52)	79.9(1)	B(24)−Mg(2)−N(61)	114.0(1)
Mg(1)−Mg(2)−B(14)	44.3(1)	B(25)−Mg(2)−N(61)	87.4(1)
Mg(1)−Mg(2)−C(21)	107.1(1)	Mg(1)−Mg(2)−N(62)	138.0(1)
B(14)−Mg(2)−C(21)	151.1(1)	B(14)−Mg(2)−N(62)	99.4(1)
Mg(1)−Mg(2)−C(22)	92.4(1)	C(21)−Mg(2)−N(62)	104.5(1)
B(14)−Mg(2)−C(22)	126.7(1)	C(22)−Mg(2)−N(62)	99.1(1)
C(21)−Mg(2)−C(22)	33.6(1)	B(23)−Mg(2)−N(62)	122.7(1)
Mg(1)−Mg(2)−B(23)	56.8(1)	B(24)−Mg(2)−N(62)	160.4(1)
B(14)−Mg(2)−B(23)	93.7(1)	B(25)−Mg(2)−N(62)	135.1(1)
C(21)−Mg(2)−B(23)	59.7(1)	N(61)−Mg(2)−N(62)	80.4(1)
C(22)−Mg(2)−B(23)	35.8(1)	Mg(1)−C(11)−C(12)	72.8(2)
Mg(1)−Mg(2)−B(24)	47.8(1)	Mg(1)−C(11)−B(15)	66.1(2)
B(14)−Mg(2)−B(24)	91.5(1)	C(12)−C(11)−B(15)	110.5(3)

Table 4 (Continued)

Compound **I**

C(21)−Mg(2)−B(24)	61.1(1)	Mg(1)−C(11)−B(16)	94.1(2)
C(12)−C(11)−B(16)	64.0(2)	Mg(1)−B(15)−B(16)	98.3(2)
B(15)−C(11)−B(16)	66.0(2)	C(11)−B(15)−B(16)	60.6(2)
Mg(1)−C(12)−C(11)	73.8(1)	B(14)−B(15)−B(16)	62.3(2)
Mg(1)−C(12)−B(13)	67.3(1)	C(11)−B(16)−C(12)	52.9(2)
C(11)−C(12)−B(13)	111.1(2)	C(11)−B(16)−B(13)	93.8(2)
Mg(1)−C(12)−B(16)	94.3(2)	C(12)−B(16)−B(13)	53.1(2)
C(11)−C(12)−B(16)	63.0(2)	C(11)−B(16)−B(14)	95.3(2)
B(13)−C(12)−B(16)	65.8(2)	C(12)−B(16)−B(14)	94.5(2)
Mg(1)−B(13)−C(12)	77.3(1)	B(13)−B(16)−B(14)	55.0(2)
Mg(1)−B(13)−B(14)	67.1(1)	C(11)−B(16)−B(15)	53.4(2)
C(12)−B(13)−B(14)	105.9(3)	C(12)−B(16)−B(15)	93.1(2)
Mg(1)−B(13)−B(16)	97.4(2)	B(13)−B(16)−B(15)	95.2(2)
C(12)−B(13)−B(16)	61.1(2)	B(14)−B(16)−B(15)	55.2(2)
B(14)−B(13)−B(16)	62.3(2)	Mg(2)−C(21)−C(22)	72.3(2)
Mg(1)−B(14)−Mg(2)	88.1(1)	Mg(2)−C(21)−B(25)	66.9(2)
Mg(1)−B(14)−B(13)	73.6(2)	C(22)−C(21)−B(25)	110.5(3)
Mg(2)−B(14)−B(13)	89.4(2)	Mg(2)−C(21)−B(26)	94.2(2)
Mg(1)−B(14)−B(15)	72.8(2)	C(22)−C(21)−B(26)	64.2(2)
Mg(2)−B(14)−B(15)	150.2(2)	B(25)−C(21)−B(26)	65.6(2)
B(13)−B(14)−B(15)	106.2(3)	Mg(2)−C(22)−C(21)	74.1(2)
Mg(1)−B(14)−B(16)	101.3(2)	Mg(2)−C(22)−B(23)	68.2(2)
Mg(2)−B(14)−B(16)	145.9(2)	C(21)−C(22)−B(23)	111.8(2)
B(13)−B(14)−B(16)	62.7(2)	Mg(2)−C(22)−B(26)	94.7(2)
B(15)−B(14)−B(16)	62.5(2)	C(21)−C(22)−B(26)	63.2(2)
Mg(1)−B(15)−C(11)	78.5(2)	B(23)−C(22)−B(26)	65.8(2)
Mg(1)−B(15)−B(14)	67.6(2)	Mg(2)−B(23)−C(22)	76.0(2)
C(11)−B(15)−B(14)	106.2(3)	Mg(2)−B(23)−B(24)	67.5(2)
C(22)−B(23)−B(24)	105.0(3)	C(21)−B(26)−B(23)	94.1(2)
Mg(2)−B(23)−B(26)	96.7(2)	C(22)−B(26)−B(23)	53.2(2)
C(22)−B(23)−B(26)	61.0(2)	C(21)−B(26)−B(24)	95.8(2)
B(24)−B(23)−B(26)	61.4(2)	C(22)−B(26)−B(24)	95.1(2)
Mg(1)−B(24)−Mg(2)	87.7(1)	B(23)−B(26)−B(24)	55.9(2)
Mg(1)−B(24)−B(23)	85.7(2)	C(21)−B(26)−B(25)	53.9(2)
Mg(2)−B(24)−B(23)	72.8(1)	C(22)−B(26)−B(25)	93.3(2)
Mg(1)−B(24)−B(25)	151.9(2)	B(23)−B(26)−B(25)	96.0(2)
Mg(2)−B(24)−B(25)	72.6(2)	B(24)−B(26)−B(25)	55.2(2)
B(23)−B(24)−B(25)	106.5(3)	Mg(1)−N(51)−C(53)	103.6(2)
Mg(1)−B(24)−B(26)	142.7(2)	Mg(1)−N(51)−C(55)	114.1(2)
Mg(2)−B(24)−B(26)	100.2(2)	Mg(1)−N(51)−C(56)	112.7(2)
B(23)−B(24)−B(26)	62.7(2)	Mg(1)−N(52)−C(54)	105.9(2)
B(25)−B(24)−B(26)	62.8(2)	Mg(1)−N(52)−C(57)	112.1(2)
Mg(2)−B(25)−C(21)	77.3(2)	Mg(1)−N(52)−C(58)	114.2(2)
Mg(2)−B(25)−B(24)	68.2(2)	Mg(2)−N(61)−C(63)	102.9(2)
C(21)−B(25)−B(24)	106.0(2)	Mg(2)−N(61)−C(65)	115.8(2)
Mg(2)−B(25)−B(26)	97.5(2)	Mg(2)−N(61)−C(66)	110.7(2)
C(21)−B(25)−B(26)	60.5(2)	Mg(2)−N(62)−C(64)	105.4(2)
B(24)−B(25)−B(26)	62.1(2)	Mg(2)−N(62)−C(67)	113.3(2)
C(21)−B(26)−C(22)	52.6(2)	Mg(2)−N(62)−C(68)	113.0(2)

Compound **II**

B(14)−B(13)−B(16)	59.3(13)	B(13)−Mg−B(13A)	90.9(4)
B(13)−Mg−B(14)	39.9(2)	B(14)−Mg−B(13A)	108.0(2)
B(13)−Mg−N(25)	105.1(2)	N(25)−Mg−B(13A)	141.3(2)
B(14)−Mg−N(25)	106.7(2)	B(13)−Mg−B(14A)	108.0(2)
B(14)−Mg−B(14A)	141.9(3)	Mg−B(14)−B(13)	66.9(3)
N(25)−Mg−B(14A)	101.4(2)	Mg−B(14)−B(15)	135.6(4)
B(13A)−Mg−B(14A)	39.9(2)	B(13)−B(14)−B(15)	102.3(5)
B(13)−Mg−N(25A)	141.3(2)	Mg−B(14)−B(16)	130.2(4)
B(14)−Mg−N(25A)	101.4(2)	B(13)−B(14)−B(16)	63.3(4)
N(25)−Mg−N(25A)	84.3(3)	B(15)−B(14)−B(16)	60.3(4)
B(13A)−Mg−N(25A)	105.1(2)	C(11)−B(15)−B(14)	103.9(5)
B(14A)−Mg−N(25A)	106.7(2)	C(11)−B(15)−B(16)	62.8(4)
C(12)−C(11)−B(15)	112.4(5)	B(14)−B(15)−B(16)	59.1(4)
C(12)−C(11)−B(16)	66.3(4)	C(11)−B(16)−C(12)	49.6(3)
B(15)−C(11)−B(16)	65.4(4)	C(11)−B(16)−B(13)	90.5(4)
C(11)−C(12)−B(13)	114.8(5)	C(12)−B(16)−B(13)	50.2(4)
C(11)−C(12)−B(16)	64.1(4)	C(11)−B(16)−B(14)	97.2(5)
B(13)−C(12)−B(16)	66.1(4)	C(12)−B(16)−B(14)	93.1(5)
C(11)−C(12)−C(24)	121.6(5)	B(13)−B(16)−B(14)	56.2(4)
B(13)−C(12)−C(24)	122.3(5)	C(11)−B(16)−B(15)	51.9(3)
B(16)−C(12)−C(24)	130.7(5)	C(12)−B(16)−B(15)	89.7(4)
Mg−B(13)−C(12)	138.2(5)	B(13)−B(16)−B(15)	97.6(5)
Mg−B(13)−B(14)	73.2(4)	B(14)−B(16)−B(15)	60.6(4)
C(12)−B(13)−B(14)	106.4(5)	Mg−N(25)−C(26)	105.1(3)
Mg−B(13)−B(16)	133.6(4)	Mg−N(25)−C(27)	114.9(4)
C(12)−B(13)−B(16)	63.7(4)	Mg−N(25)−C(28)	111.4(3)
B(14)−B(13)−B(16)	60.4(4)		

Table 4 (Continued)

Compound **IV**

C(11)−Mg−C(12)	35.8(5)	C(12)−Mg−B(13)	37.1(5)
C(11)−Mg−B(13)	62.8(5)	C(11)−Mg−B(14)	63.9(5)
C(12)−Mg−B(14)	64.1(5)	Mg−C(11)−C(12)	72.6(7)
B(13)−Mg−B(14)	41.2(6)	Mg−C(11)−B(15)	69.7(8)
C(11)−Mg−B(15)	37.8(6)	C(12)−C(11)−B(15)	109.6(12)
C(12)−Mg−B(15)	62.3(5)	Mg−C(11)−B(16)	95.3(8)
B(13)−Mg−B(15)	65.6(6)	C(12)−C(11)−B(16)	62.1(10)
B(14)−Mg−B(15)	38.7(6)	B(15)−C(11)−B(16)	65.0(10)
B(13)−Na−B(14)	33.6(5)	Mg−C(12)−C(11)	71.6(7)
B(13)−Na−B(16)	33.7(5)	Mg−C(12)−B(13)	70.0(8)
B(14)−Na−B(16)	34.8(5)	C(11)−C(12)−B(13)	111.8(12)
B(13)−Na−O(31)	91.1(7)	Mg−C(12)−B(16)	96.1(9)
B(14)−Na−O(31)	110.7(7)	C(11)−C(12)−B(16)	65.3(10)
B(16)−Na−O(31)	123.8(7)	B(13)−C(12)−B(16)	65.5(10)
B(13)−Na−O(312)	97.3(6)	Mg−B(13)−Na	136.5(7)
B(14)−Na−O(312)	108.0(6)	Mg−B(13)−C(12)	72.9(8)
B(16)−Na−O(312)	130.9(6)	Na−B(13)−C(12)	130.8(10)
O(31)−Na−O(312)	17.1(8)	Mg−B(13)−B(14)	68.7(8)
B(13)−Na−O(41)	102.5(5)	Na−B(13)−B(14)	69.7(8)
B(14)−Na−O(41)	129.2(5)	C(12)−B(13)−B(14)	105.0(12)
B(16)−Na−O(41)	95.6(5)	Mg−B(13)−B(16)	95.6(9)
O(31)−Na−O(41)	85.6(7)	Na−B(13)−B(16)	75.7(8)
O(312)−Na−O(41)	99.8(6)	C(12)−B(13)−B(16)	60.7(10)
B(13)−Na−C(42)	108.7(7)	B(14)−B(13)−B(16)	62.2(10)
B(14)−Na−C(42)	122.8(7)	Mg−B(14)−Na	144.5(8)
B(16)−Na−C(42)	88.6(7)	Mg−B(14)−B(13)	70.1(8)
O(31)−Na−C(42)	109.2(8)	Na−B(14)−B(13)	76.7(8)
O(312)−Na−C(42)	121.5(8)	Mg−B(14)−B(15)	70.9(9)
O(41)−Na−C(42)	24.9(6)	Na−B(14)−B(15)	131.9(10)
B(13)−B(14)−B(15)	105.3(13)	C(11)−B(16)−C(12)	52.7(9)
Mg−B(14)−B(16)	95.5(9)	Na−B(16)−B(13)	70.7(8)
Na−B(14)−B(16)	78.4(8)	C(11)−B(16)−B(13)	93.8(11)
B(13)−B(14)−B(16)	60.4(10)	C(12)−B(16)−B(13)	53.8(9)
B(15)−B(14)−B(16)	63.3(10)	Na−B(16)−B(14)	66.8(7)
Mg−B(15)−C(11)	72.5(8)	C(11)−B(16)−B(14)	94.1(11)
Mg−B(15)−B(14)	70.4(9)	C(12)−B(16)−B(14)	96.4(11)
C(11)−B(15)−B(14)	108.2(13)	B(13)−B(16)−B(14)	57.4(10)
Mg−B(15)−B(16)	95.3(10)	Na−B(16)−B(15)	113.7(10)
C(11)−B(15)−B(16)	61.6(10)	C(11)−B(16)−B(15)	53.4(9)
B(14)−B(15)−B(16)	63.5(10)	C(12)−B(16)−B(15)	93.6(11)
Na−B(16)−C(11)	159.7(10)	B(13)−B(16)−B(15)	95.7(11)
Na−B(16)−C(12)	120.2(10)	B(14)−B(16)−B(15)	53.2(10)

a drybox, coated with mineral oil, and sequentially mounted on a Siemens R3m/V diffractometer under a low-temperature nitrogen stream. The pertinent crystallographic data and conditions for data collection are summarized in Table 3. Final unit cell parameters were obtained by a least-squares fit of the angles of 24−30 accurately centered reflections in the 2θ range from 16° to 32.0°. Intensity data were corrected for Lorentz and polarization effects. The structures were solved by direct methods using the SHELXTL-*Plus* package and subsequent Fourier syntheses.[17] Full-matrix least-squares refinements were performed for all three structures. Scattering factors and anomalous-dispersion corrections for the heavy atoms were taken from ref 18. All non-H atoms, except for the C and O atoms of the disordered THF groups in **IV**, were refined isotropically. Bonds in the disordered groups were restrained during the final cycles of refinements. Methyl and methylene H's in the nondisordered groups were placed in calculated positions. The cage H's of **I** were isotropically refined, while those of **II** and **IV** were located in DF maps but were not refined. The final values of R and R_w are listed in Table 3, while selected bond lengths and bond angles are given in Table 4. The atomic coordinates, a full list of bond lengths and angles, isotropic thermal parameters, and positions of the H atoms are given in the Supporting Information.

Calculations. The ^{11}B NMR spectra of compounds **I**−**VII** were analyzed with the aid of GIAO (gauge-independent atomic orbital)[19] ab initio molecular orbital calculations at the HF/6-311G** level of theory on the model compounds *closo*-1-(en)-1,2,3-$MgC_2B_4H_6$ (**VIII**), *commo-exo*-4,4′,5,5′-Mg(en)-[2,3-$C_2B_4H_7$]$_2$ (**IX**), *closo*-1-(en)-1,2,4-$MgC_2B_4H_6$ (**X**), {*commo*-1,1′-[1,2,3-$MgC_2B_4H_6$]$_2$}$^-$ (**XI**), and {*commo*-1,1′-[1,2,4-$MgC_2B_4H_6$]$_2$}$^-$ (**XII**) (en = ethylenediamine, $(NH_2CH_2)_2$). These compounds differ from their **I**−**VII** analogues in that H's replace the $SiMe_3$ groups on the cage carbons and en is used in place of TMEDA as the metal-solvating group. Such substitutions have been successfully used in generating model systems for interpreting the ^{11}B NMR spectra of a number of trimethylsilyl-substituted carboranes and metallacarboranes.[20,21] The structures of the model compounds were optimized by approximate density function theory (DFT) using Becke's three-parameter method[22] and the correlation functional of Lee, Yang, and Parr[23] with the 6-31G* basis set (B3LYP/6-31G*).[24] The GIAO−HF/6-311G**//B3LYP/6-31G* calculations were carried out on a Dec-αA or a Silicon Graphics Indigo2 Impact10000 workstation using the Gausian 94 series of programs.[25] The ^{11}B chemical shifts calculated for the model compounds, listed in Table 5,

(17) Sheldrick, G. M. *Structure Determination Software Programs;* Siemens X-ray Analytical Instrument Corp.: Madison, WI, 1991.

(18) *International Tables For X-ray Crystallography;* Kynoch press: Birmingham, U.K., 1974; Vol. IV.

(19) Wolinski, K.; Hilton, J. F.; Pulay, P. *J. Am. Chem. Soc.* **1990**, *112*, 8251.

(20) Ezhova, M. B.; Zhang, H.; Maguire, J. A.; Hosmane, N. S. *J. Organomet. Chem.*, in press.

(21) Hosmane, N. S.; Lu, K.-J.; Zhang, H.; Maguire, J. A. *Organometallics* **1997**, *16*, 5163.

(22) Becke, A. D. *J. Chem. Phys.* **1993**, *98*, 5648.

(23) Lee, C.; Yang, W.; Parr, R. G. *Phys. Rev. B* **1988**, *37*, 785.

(24) For a discussion of DFT methods, see: Ziegler, T. *Chem. Rev.* **1991**, *91*, 651 and references therein.

Table 5. Calculated ^{11}B NMR Chemical Shifts of Some Magnesacarboranes[a]

compound	δ, ppm[b,c] basal[d]	unique[e]	apical[f]
closo-1-(en)-1,2,3-$MgC_2B_4H_6$ (**VIII**)	13.67 (2)	8.88 (1)	−49.62 (1)
commo-exo-4,4′,5,5′-Mg(en)-[2,3-$C_2B_4H_6$]$_2$ (**IX**)[g]	5.44 (1) 4.35 (1)	−4.24 (1)	−52.48 (1)
closo-1-(en)-1,2,4-$MgC_2B_4H_6$ (**X**)	14.82 (1)	10.84 (2)	−48.52 (1)
{*commo*-1,1′-[1,2,3-$MgC_2B_4H_6$]$_2$}$^{2-}$ (**XI**)	11.61 (2)	0.69 (1)	−54.80 (1)
{*commo*-1,1′-[1,2,4-$MgC_2B_4H_6$]$_2$}$^{2-}$ (**XII**)	12.35 (1)	5.90 (2)	−55.09 (1)
closo-[1,2,4-$LiC_2B_4H_6$]$^-$ [h]	12.87 (1)	9.81 (2)	−49.84 (1)
closo-[1,2,3-$LiC_2B_4H_6$]$^-$ [h]	15.48 (2)	6.59 (1)	−49.02 (1)
closo-exo-5,6(μ-H_2)$_2$Li-1,2,3-$LiC_2B_4H_6$][h,i]	16.25 (1) 8.52 (1,BLi)	3.83 (1)	−48.76 (1)

[a] Geometries optimized at the B3LYP/6-31G* level. [b] GIAO-calculated chemical shifts at the HF/6-311G** level, realtive to BF_3·OEt_2 calculated at the same level. [c] Relative areas in parentheses. [d] Equivalent to B(13,15) in Figures 1−3. [e] Equivalent to B(14) in Figures 1−3. [f] Equivalent to B(16) in Figures 1−3. [g] The order is B(13), B(15), B(14), and B(16) in Figure 2. [h] From ref 20. [i] The sequence in order of increasing shielding is B(basal, no bridge), B(basal, Li bridge), B(unique), B(apical).

Scheme 1. Syntheses of Half- and Full-Sandwich Magnesacarboranes of the C_2B_4-Cage Systems

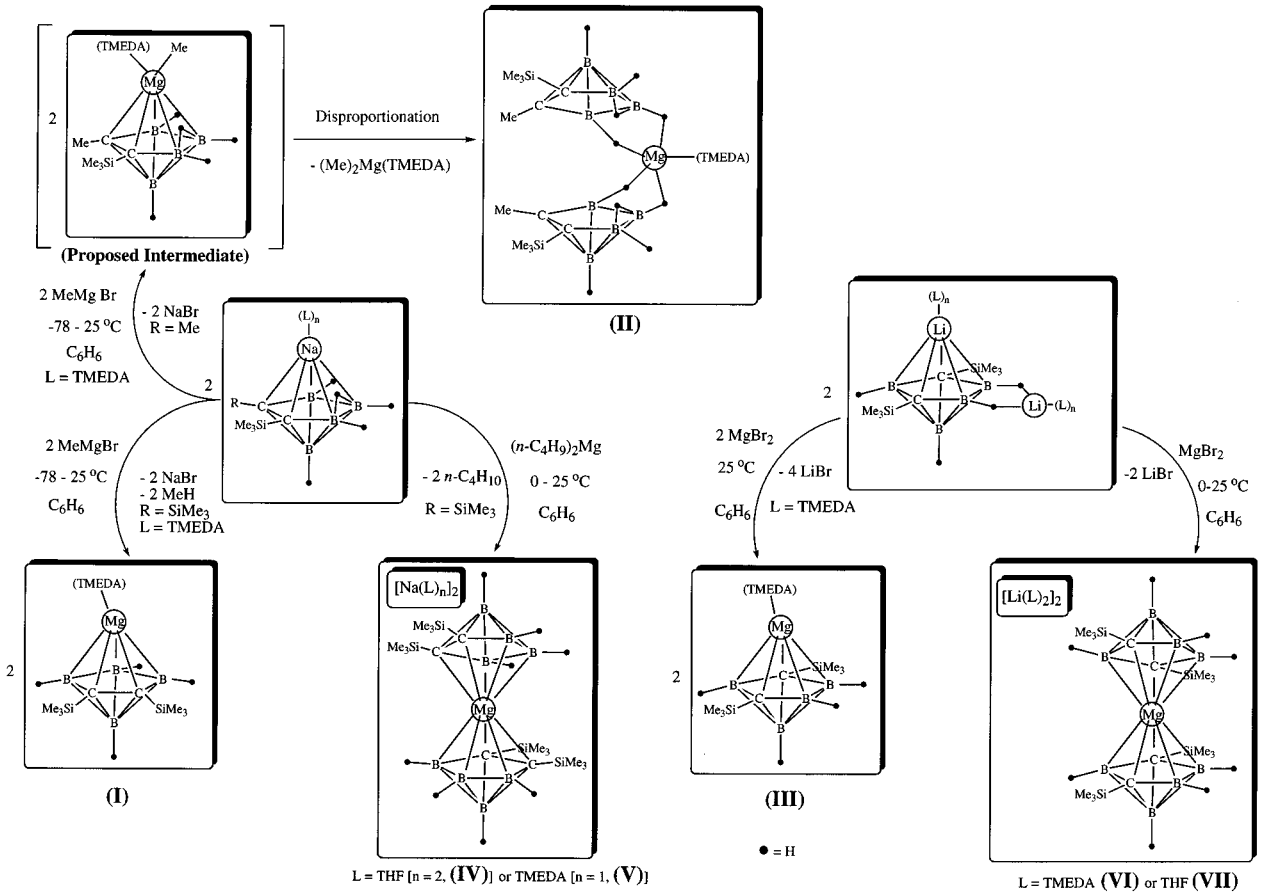

are relative to BF_3·OEt_2 as a standard. The standard was subjected to the same optimization/GIAO cycle as were the compounds.

Results and Discussion

Synthesis. The magnesacarboranes were prepared by the reactions of either the carbons-adjacent monosodium carboranes *nido*-1-Na(L)$_n$-2-($SiMe_3$)-3-(R)-2,3-$C_2B_4H_5$ (n = 2, L =THF, R = $SiMe_3$; n = 1, L = TMEDA, R = $SiMe_3$ or Me) or the carbons-apart dilithium compounds *closo-exo*-5,6-[(μ-H)$_2$Li(L)$_n$]-1-Li(L)$_n$-2,4-($SiMe_3$)$_2$-2,4-$C_2B_4H_4$ (n = 2, L = THF; n = 1, L = TMEDA) with various metalating reagents, as outlined in Scheme 1. As can be seen from this scheme, the products of these reactions are complex functions of the stoichiometries of the reactions, the nature of the carborane precursors, and the nature of the metalating reagents. The most straightforward results are those obtained from the reactions of the TMEDA-solvated dilithium carborane [Li(TMEDA)]$_2$[2,4-($SiMe_3$)$_2$-2,4-$C_2B_4H_4$] and $MgBr_2$, where the products were determined by the stiochiomtery of the reactions. A 1:1 $MgBr_2$-to-carborane molar ratio produced, in 73% yield, the half-sandwich magnesacarborane *closo*-1-Mg(TMEDA)-2,4-($SiMe_3$)$_2$-2,4-$C_2B_4H_4$ (**III**), while a 1:2 $MgBr_2$-to-carborane molar ratio gave the full-sandwich compound [*commo*-1,1′-Mg-{2,4-($SiMe_3$)$_2$-2,4-$C_2B_4H_4$}$_2$]$^{2-}$ (**VI**)

(25) Frisch, M. J.; Trucks, G. W.; Schlegel, H. B.; Gill, P. M. W.; Johnson, B. G.; Robb, M. A.; Cheeseman, J. R.; Keith, T.; Peterson, G. A.; Montgomery, J. A.; Raghavachari, K.; Al-Laham, M. A.; Zakrzewski, V. G.; Ortiz, J. V.; Foresman, J. B.; Peng, C. Y.; Ayala, P. Y.; Chen, W.; Wong, M. W.; Andres, J. L.; Replogle, E. S.; Gomperts, R.; Martin, R. L.; Fox, D. J.; Binkley, J. S.; Defrees, D. J.; Baker, J.; Stewart, J. P.; Head-Gordon, M.; Gonzalez, C.; Pople, J. A. *Gaussian 94*, Revision D.4; Gaussian, Inc.: Pittsburgh, PA, 1995.

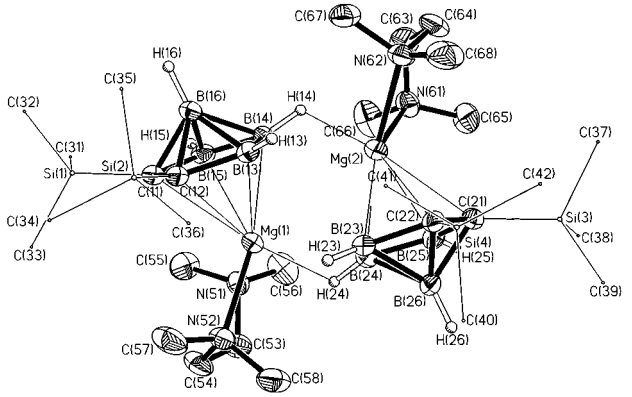

Figure 1. A perspective view of the "carbons adjacent" dimeric magnesacarborane half-sandwich, *closo*-1-Mg(TMEDA)-2,3-$(SiMe_3)_2$-2,3-$C_2B_4H_4$ (**I**), showing the atom-numbering scheme. The thermal ellipsoids are drawn at the 40% probability level. For clarity, the *exo*-polyhedral $SiMe_3$ groups were drawn with circles of arbitrary radii and the methyl and methylene H's are omitted.

in 85% yield. It is not obvious what specific interactions determine the product distributions in these reactions. The driving force for the formation of the half-sandwich magnesacarborane, **III**, could well be the removal from solution of the insoluble LiBr coproduct which forms along with the metallacarborane. However, the formation of the full-sandwich complex, **VI**, which involves, at least formally, the displacement of a TMEDA molecule on **III** by a carborane dianion is not accompanied by the formation of an insoluble coproduct. Thus, the *commo*-magnesacarborane, **VI**, seems to be an inherently very stable compound whose formation drives the reaction essentially to completion (85% yield). In a similar manner, the full-sandwich carbons-adjacent *commo*-magnesacarboranes, **IV** and **V**, were produced in high yields (82% and 85%, respectively) from a 1:2 stoichiometry of the dialkylmagnesium with either the THF-(**IV**) or the TMEDA-solvated (**V**) monosodium compounds of the [2,3-$(SiMe_3)_2$-2,3-$C_2B_4H_5]^-$ monoanion.

While the results of the reactions of the mono- and dianions of the carboranes with either the magnesium dialkyl or the magnesium dihalide reagents can be readily rationalized, the reactions with the mixed-alkyl/halide Grignard reagent, MeMgBr, are more difficult to explain. The half-sandwich magnesacarborane *closo*-1-Mg(TMEDA)-2,3-$(SiMe_3)_2$-2,3-$C_2B_4H_4$ (**I**) was formed from the 1:1 molar ratio reaction of the Grignard reagent with [Na(TMEDA)][2,3-$(SiMe_3)_2$-2,3-$C_2B_4H_5$]. The solid-state structure of **I** shows it to be a dimer of two opposing half-sandwich magnesacarboranes in which a TMEDA-solvated Mg occupies the apical position above the C_2B_3 face of one carborane and is bonded to the unique boron of the other carborane through a Mg−H−B bridge (see Figure 1). Two coproducts, insoluble NaBr and gaseous CH_4, are formed along with the dimer. Although it is experimentally impossible to determine which coproduct forms first, a reasonable sequence would be the initial formation of NaBr and an alkyl-substituted magnesacarborane of the form *closo*-1-(TMEDA)Mg(CH_3)-2,3-$(SiMe_3)_2$-2,3-$C_2B_4H_5$, which would then dimerize with the elimination CH_4. This sequence is supported by ab initio molecular orbital calculations on the model system 1-(en)Mg(CH_3)-2,3-$C_2B_4H_5$ [en = $(NH_2CH_2)_2$]. Molecular orbital calculations at the HF-3-21G* level of theory show the methylmagnesacarborane to be a stable compound whose decomposition, according to eq 1, would be exothermic, with a calculated $\Delta E = -55.5$ kJ/mol. While this energy change must be viewed with some caution, it does suggest that the assumption of a kinetically formed intermediate is not unreasonable. Similar intermediates are thought to be important in the other magnesacarborane formation reactions (vide infra). One of the most surprising results in this study was the formation of the exo-sandwich magnesacarborane *commo-exo*-4,4′,5,5′-Mg(TMEDA)[2-($SiMe_3$)-3-(Me)-2,3−$C_2B_4H_5]_2$ (**II**), from the reaction of MeMgBr with [Na(TMEDA)][2-($SiMe_3$)-3-(Me)-2,3-$C_2B_4H_5$] under conditions identical to those used in the synthesis of the *closo*-magnesacarborane **I**. This compound was produced in 94% yield, the highest for any magnesacarborane, from a 1:1 Grignard-to-carborane molar ratio. Scheme 1 outlines our tentative rationalization for this reaction. As in the formation of **I**, we postulate that the initial product in the reaction is the methylmagnesacarborane *closo*-1-(TMEDA)Mg(CH_3)-2-($SiMe_3$)-3-(Me)-2,3−$C_2B_4H_5$. This intermediate, instead of dimerizing with the loss of methane, undergoes a disproportionation reaction to give **II** and a dialkylmagnesium compound (see Scheme 1) through a Schlenk-type of equilibrium,[26] as shown in eq 2. The postulated $(Me)_2$Mg(TMEDA) product was

$$1\text{-(en)Mg(CH}_3\text{)-2,3-C}_2\text{B}_4\text{H}_5 \rightarrow 1\text{-(en)Mg-2,3-C}_2\text{B}_4\text{H}_4 + \text{CH}_4 \quad (1)$$

$$2[1\text{-(TMEDA)Mg(CH}_3\text{)-2-(SiMe}_3\text{)-3-(Me)-2,3-C}_2\text{B}_4\text{H}_5] \rightleftharpoons 4,4',5,5'\text{-Mg(TMEDA)-[2-(SiMe}_3\text{)-3-(Me)-2,3-C}_2\text{B}_4\text{H}_5]_2\ (\mathbf{II}) + (Me)_2\text{Mg(TMEDA)} \quad (2)$$

reported to be soluble in benzene and would remain in solution when **II** was recrystallized from that solvent.[27] Irrespective of the mechanism, the almost quantitative formation of **II** shows that it is an extremely stable compound. The formation of the exo-sandwich magnesacarborane instead of a more conventional closo-product, similar to **I**, could be the result of less steric crowding in the initially formed *closo*-methylmagnesacarborane intermediate, which in turn would allow dimerization directly between the two capping magnesium atoms *via* a double Me and carborane bridge. Such doubly bridged structures have been proposed as transition states in the ligand exchange processes that proceed through Schlenk equilibria.[27] In the formation of **I**, the presence of the second bulky $SiMe_3$ group could prevent such bridging and restrict interaction of the two methylmagnesacarborane intermediates to the sides opposite the cage carbons as found in **I** (see Figure 1).

A half-sandwich methylmagnesacarborane intermediate may also play a role in the sequential reaction of the Grignard reagent with equimolar amounts of first

(26) For references and discussion of Schlenk equilibria, see: (a) Linsell, W. E. In *Comprehensive Organometallic Chemistry I*; Abel, E. W., Stone, F. G. A., Wilkinson, G., Eds.; Pergamon: Oxford, 1982; Vol. 1. (b) Linsell, W. E. In *Comprehensive Organometallic Chemistry II*; Abel, E. W., Stone, F. G. A., Wilkinson, G., Eds.; Elsevier: New York, 1995; Vol. 1.

(27) Coates, G. E.; Heslop, J. A. *J. Chem. Soc. A* **1966**, 26.

$[Li(THF)_2]_2[2,4\text{-}(SiMe_3)_2\text{-}2,4\text{-}C_2B_4H_4]$ and then $[Na(THF)_2][2,3\text{-}(SiMe_3)_2\text{-}2,3\text{-}C_2B_4H_5]$. The reaction did not produce the expected mixed-ligand carborane sandwich compound; instead, a 50:50 mixture of the carbons-apart and carbons-adjacent full-sandwich magnesacarboranes, $[Li(THF)_2]_2[commo\text{-}1,1'\text{-}Mg\{2,4\text{-}(SiMe_3)_2\text{-}2,4\text{-}C_2B_4H_4\}_2]$ (**VII**) and $[Na(THF)_2]_2[commo\text{-}1,1'\text{-}Mg\{2,3\text{-}(SiMe_3)_2\text{-}2,3\text{-}C_2B_4H_4\}_2]$ (**IV**) was obtained, in yields of 88% and 79%, respectively. There has been one reported synthesis of a mixed-ligand metallacarborane, that of the dimeric erbacarborane $\{[Li(TMEDA)_2]_2[commo\text{-}1\text{-}(2,3\text{-}(SiMe_3)_2\text{-}2,3\text{-}C_2B_4H_4)\text{-}1\text{-}Er\text{-}(2,4\text{-}(SiMe_3)_2\text{-}2,4\text{-}C_2B_4H_4)]\}_2$, which was formed in 95% yield from the reaction of the carbons-adjacent, full-sandwich erbacarborane with the dilithium compound $[Li(TMEDA)]_2[2,4\text{-}(SiMe_3)_2\text{-}2,4\text{-}C_2B_4H_4]$.[28] In view of this result, there seems little reason to assume that the mixed−ligand metallacarborane would be inherently less stable than its homoligated analogues. A plausible explanation for the exclusive formation of **IV** and **VII** involves the initial formation of a carbons-apart *closo*-methylmagnesacarborane that exists in equilibrium with **IV** and a THF-solvated dimethylmagnesium product. In a reaction similar to that observed for $Mg(Bu)_2$, the dimethylmagnesium compound could react irreversibly with the bridged hydrogens of $[Na(THF)_2][2,3\text{-}(SiMe_3)_2\text{-}2,3\text{-}C_2B_4H_5]$ to give **VII** and gaseous methane. Thus, the various products found in the study of the reaction of the Grignard reagent, MeMgBr, with different carboranes can be rationalized, although not predicted, by assuming the initial formation of a *closo*-methylmagnesacarborane intermediate, which, depending on the nature of the carborane and the metal-solvating molecules, could further react to produce compounds **I**, **II**, **IV**, or **VII**.

Crystal Structures of *closo*-1-Mg(TMEDA)-2,3-$(SiMe_3)_2$-2,3-$C_2B_4H_4$ (I), *commo-exo*-4,4′,5,5′-Mg(TMEDA)$_2$[2-$(SiMe_3)$-3-(Me)-2,3-$C_2B_4H_5$]$_2$ (II), and $[Na(THF)_2]_2$-[*commo*-1,1′-Mg{2,3-$(SiMe_3)_2$-2,3-$C_2B_4H_4$}$_2$] (IV). The crystal structures of the magnesacarboranes **I**, **II**, and **IV** are shown in Figures1−3, respectively; some important bond distances and angles are given in Table 4. Figure 1 shows that compound **I** crystallizes as a dimer of two oppositely oriented *closo*-1-Mg(TMEDA)-2,3-$(SiMe_3)_2$-2,3-$C_2B_4H_4$ half-sandwich complexes. As described earlier, each magnesium occupies an apical position above an open C_2B_3 pentagonal face of one carborane unit and is bonded to the unique boron of the other carborane *via* a Mg−H−B bridge. The relevant bond distances in Figure 1, in Å, are Mg(1,2)−C(11,21) = 2.649(3), 2.621(4); Mg(1,2)−C(12,22) = 2.635(3), 2.596(3); Mg(1,2)−B(13,23) = 2.493(3), 2.485(3); Mg(1,2)−B(15,25) = 2.472(4), 2.471(3); Mg(1,2)−B(14,24) = 2.393(3), 2.404(3). Although some variations exist, the structures of both complexes are essentially equivalent in that each capping magnesium atom resides in the pseudomirror plane of its respective carborane ligand,[29] but is displaced slightly away from the cage carbons and toward the unique borons of each cage, borons B(14) and B(24) in Figure 1. These distortions result in metal−cage carbon distances that are about 0.1−0.3 Å longer than the metal−boron distances. Similar slip distortions were found in the full- and half-sandwich group 13 and group 14 metallacarboranes and have been attributed to preferential bonding with the borons by the metal p orbitals oriented tangentially to the cage.[1] Since the p orbitals on the magnesium would be very diffuse, it is doubtful that such interactions play a major role in the distortions

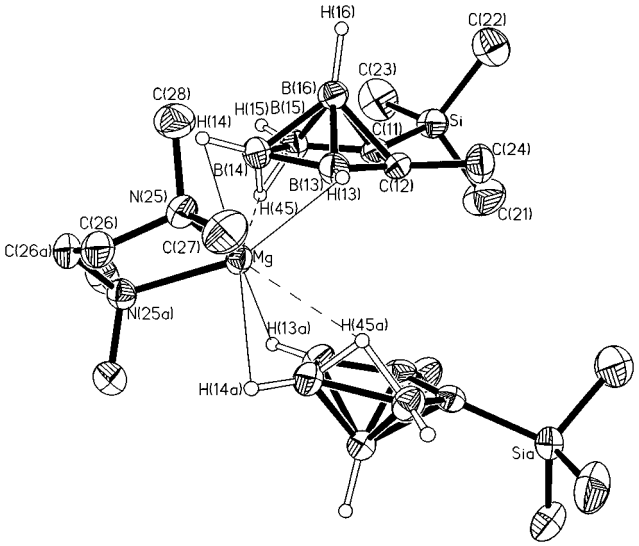

Figure 2. A perspective view of the *exo*-sandwich magnesacarborane, *commo-exo*-4,4′,5,5′-Mg(TMEDA)$_2$[2-$(SiMe_3)$-3-(Me)-2,3-$C_2B_4H_5$]$_2$ (**II**), showing the atom-numbering scheme. The thermal ellipsoids are drawn at the 40% probability level. For clarity, the methyl and methylene H's are omitted.

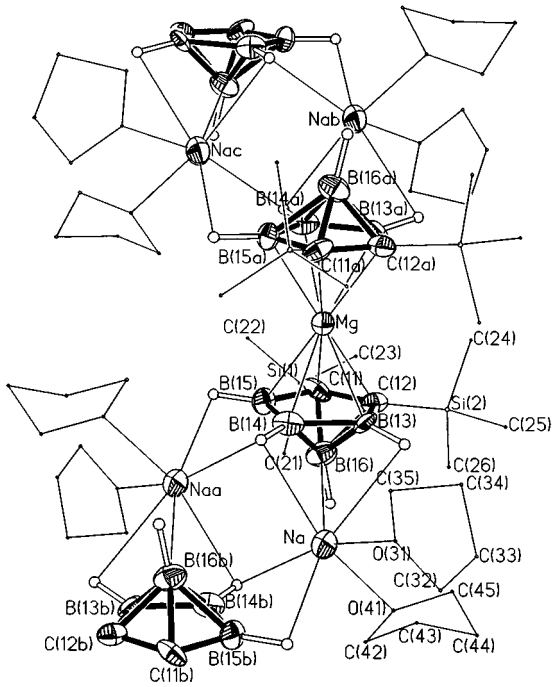

Figure 3. A perspective view of the polymeric full-sandwich magnesacarborane, $[Na(THF)_2]_2$-[*commo*-1,1′-Mg-$\{2,3\text{-}(SiMe_3)_2\text{-}2,3\text{-}C_2B_4H_4\}_2$] (**IV**), showing the atom-numbering scheme. The thermal ellipsoids are drawn at the 40% probability level. For clarity, the solvated THF molecules and the *exo*-polyhedral $SiMe_3$ units are drawn with circles of arbitrary radii.

(28) Hosmane, N. S.; Wang, Y.; Zhang, H.; Oki, A. R.; Maguire, J. A.; Waldhör, E.; Kaim, W.; Binder, H.; Kremer, R. K. *Organometallics* **1995**, *14*, 1101.

(29) In Figure 1, the plane containing the apical borons (B(16) and B(26)), the unique borons (B(14) and B(24)), and the midpoint of the bond between the cage carbons.

seen in Figure 1. They are most probably related to the rather strong interaction of each magnesium with the unique boron on the opposing cage; these distances are Mg(1,2)−B(24,14) = 2.540(5) Å, 2.534(5), which are significantly shorter than the Mg−C(cage) distances in each complex. Support for this explanation is found in the structure of the full−sandwich magnesacarborane **IV**. Inspection of the equivalent Mg−C_2B_3 bond distances in **IV**, as shown in Figure 3 and listed in Table 4, provides no evidence for a slip distortion; the two carborane ligands are equivalent and are η^5-bonded to the commo-magnesium metal, with the average Mg−C_2B_3 bond distances being 2.426 ± 0.022 Å.[30] In contrast to the very symmetric bonding in **IV**, the exo-sandwich magnesacarborane **II** shows such extreme slippage that the compound is better described as one in which a TMEDA-solvated magnesium is exo-polyhedrally bound to the two cages through a pair of Mg−H−B bridges of unequal strength. The pertinent bond distances are Mg−B(13) = 2.383(8) Å; Mg−B(14) = 2.480(7) Å (see Figure 2). These distances are comparable to the shorter metal−carborane atom bond distances in compounds **I** and **IV** (see Table 4). The attenuated metal−cage bonding in **II** is somewhat compensated by stronger bonding by the TMEDA. The Mg−N bond distances in **II** are 2.183 Å, compared to average distances of 2.290 ± 0.036 Å in **I**.

Due to the severe disorder of the solvating TMEDA molecules the structure of the carbons-apart full-sandwich compound, **VI**, could not be completely refined.[31] However, a full−sandwich magnesacarborane, more similar to **IV** than to **II**, was clearly evident from the difference Fourier maps. This structure is consistent with its analytical and spectroscopic data.

Spectra. Compounds **I**−**VII** were characterized by their ^{1}H, ^{11}B, and ^{13}C NMR spectra, with **VII** being further characterized by its ^{7}Li NMR spectrum (see Table 1). The spectra show resonances consistent with the formulations given in the Experimental Section and, in the cases of compounds **I**, **II**, and **IV**, with their solid-state crystal structures. The ^{11}B NMR spectra of other main-group metallacarboranes in the C_2B_4 cage system have proven especially useful as characterization tools. In general, the group 1 mono- and dianionic carborane precursors of **I**−**VII** all show a resonance in the δ −50 ppm range due to the apical boron (B(16) in Figures 1−3), with the resonances of the less-shielded borons of the C_2B_3 open faces being shifted downfield by some 50−80 ppm.[7] The main difference in the two systems lies in the relative positions of the unique and basal boron resonances.[32] In the carbons-adjacent carboranes, the basal borons are the least shielded and a 2:1:1 peak area ratio pattern is found,[7b] while in the carbons-apart system, the relative shieldings are reversed, which results in a 1:2:1 pattern.[7c] For example, the ^{11}B NMR spectrum of [Na(TMEDA)][2,3-($SiMe_3$)$_2$-2,3-$C_2B_4H_5$] shows three resonances of 2:1:1 peak area ratios at δ 15.68, 1.92 and −49.73 ppm,[7b] while a 1:2:1 pattern at δ 18.02, 6.56, and −48.78 ppm is found for *closo-exo*-5,6-[(μ-H)$_2$Li(TMEDA)]-1-Li(TMEDA)-2,4-($SiMe_3$)$_2$-2,4-$C_2B_4H_4$.[7c] Substitution of a group 1 metal with a more covalently bonding metal group incorporating a group 13 or 14 metal generally leads to a significant downfield shift of the apical boron resonance, with the facial borons being less affected.[33] This has been rationalized on the basis of withdrawal of total electron density from the cage to the capping metal.[34] However, the general 2:1:1 and 1:2:1 peak area ratios are maintained for the respective carbons-adjacent and carbons-apart metallacarcoranes, although the three facial boron resonances sometimes cannot be resolved, which results in 3:1 patterns.[33b,35] With the exception of **IV**, the peak area ratios found in the ^{11}B NMR spectra of magnesacarboranes, shown in Table 1, all show the expected patterns, with the 2,3-C_2B_4-based magnesacarboranes (**I**, **II**, and **V**) having 2:1:1 patterns and those based on the carbons-apart cages (**III**, **VI**, and **VII**) having 1:2:1 patterns. However, several questions arise regarding the ^{11}B NMR spectra of the magnesacarboranes. The 2:1:1 pattern found in the ^{11}B NMR spectra of **III** is surprising in view of its solid-state structure (see Figure 2), which clearly shows nonequivalent basal borons, one [B(15)] involved in a B−H−B bridge bond while the other [B(13)] is participating in a BH−Mg−BH bridge. On the other hand, the ^{11}B NMR spectra of **IV** shows a 1:1:1:1 pattern indicating nonequivalent borons, even though Figure 3 shows equivalency or at least near equivalency of the basal borons [B(13,15)]. The spectrum of **IV** also differs significantly from that of **V**, which is formulated to have the same commo-structure as that of **IV**; the only difference in these two compounds is in the nature of the molecules that solvate the sodium counterions. Since the ^{11}B NMR chemical shifts are determined by internal cage bonding, it is surprising that such a minor change in the counterions would cause that much of a difference in their spectra, especially in view of the fact that similar differences found in **VI** and **VII** produced almost no effect on their spectra (see Table 1).

In an effort to assess the changes expected in the ^{11}B NMR spectra of the metallacarboranes on substituting a magnesium for a lithium or sodium, the ^{11}B NMR shielding constants for the model compounds *closo*-1-(en)-1,2,3-$MgC_2B_4H_6$ (**VIII**), *commo-exo*-4,4′,5,5′-Mg(en)-[2,3-$C_2B_4H_6$]$_2$ (**IX**), *closo*-1-(en)-1,2,4-$MgC_2B_4H_6$ (**X**), {*commo*-1,1′-[1,2,3-$MgC_2B_4H_6$]$_2$}$^{2-}$ (**XI**), and {*commo*-1,1′-[1,2,4-$MgC_2B_4H_6$]$_2$}$^{2-}$ (**XII**) (en = ethylenediamine, (NH_2CH_2)$_2$] were determined using GIAO-HF/6-311G**//B3LYP/6-31G* molecular orbital calculations; the results are listed in Table 5. Also shown in this table are some calculated chemical shifts for several lithiacarboranes taken from ref 20. The calculated ^{11}B NMR

(30) Whenever an average value of a parameter is given, the indetermination listed is the average deviation.

(31) Compound **VI** crystallized in the monoclinic space group C2 with a = 17.685 Å, b = 14.358 Å, c = 19.952 Å, and β = 93.59°. Because of disorder, the cage could only be partially refined and the data are not included.

(32) Following normal usage, the facial boron that resides in the pseudomirror plane of the cage is the unique boron (B(14) in Figures 1−3), with the basal borons being the two off-plane atoms.

(33) (a) Hosmane, N. S.; Saxena, A. K.; Lu, K.-J.; Maguire, J. A.; Zhang, H.; Wang, Y.; Thomas, C. J.; Zhu, D.; Grover, B. R.; Gray, T. G.; Eintracht, J. F.; Isom, H.; Cowley, A. H. *Organometallics* **1995**, *14*, 5104. (b) Cowley, A. H.; Galow, P.; Hosmane, N. S.; Jutzi, P.; Norman, N. C. *J. Chem. Soc., Chem. Commun.* **1984**, 1564. (c) Hosmane, N. S.; Sirmokadam, N. N.; Herber, R. H. *Organometallics* **1984**, *3*, 1665. (d)Hosmane, N. S.; Jia, L.; Zhang, H.; Maguire, J. A. *Organometallics* **1994**, *13*, 1411.

(34) Maguire, J. A.; Ford, G. P.; Hosmane, N. S. *Inorg. Chem.* **1988**, *27*, 3354.

(35) Hosmane, N. S.; de Meester, P.; Maldar, N. N.; Potts, S. B.; Chu, S. S. C. *Organometallics* **1986**, *5*, 772.

chemical shifts of the model compounds show the expected general pattern, that is the carbons-adjacent magnesacarboranes, **VIII** and **XI**, show 2:1:1 peak area ratio patterns while their carbons-apart analogues, **X** and **XII**, exhibit 1:2:1 patterns. A comparison of the experimental chemical shifts of the apical boron resonances of **I**−**VII**, and those of the model compounds with their respective group 1 precursors shows very little change when replacing the group 1 metal with magnesium. This is in marked contrast to the changes observed for the group 13 and group 14 metallacarboranes and most likely reflects the predominately ionic interactions between the carboranes and the s-block elements. The calculated ^{11}B chemical shifts for **IX**, which is a model for **III**, show that the chemical shift of the boron involved in B−H−B bridging is very similar to that of the boron participating in Mg bridge bonding; the calculated chemical shifts are δ 4.35 and 5.44 ppm, respectively (see Table 5). Therefore, the broadened 2:1:1 pattern, as exhibited by **II**, is quite consistent with its solid-state structure (see Table 1 and Figure 2). A comparison of the chemical shifts of **I** with those of **VIII** shows a large difference in the positions of the unique boron resonances, with that of **I** (δ −0.28 ppm) being significantly upfield from that of its model compound (δ 8.88 ppm). This discrepancy is larger than can be accounted for by the substitutions made in the model compound and reflects the effects of dimerization; bridge bonding by either a H or a metal leads to deshielding. The ^{11}B NMR chemical shifts of **X**, **XI**, and **XII** agree quite well with the spectra of their respective trimethylsilyl-substituted analogues **III**, **V**, and **VI** or **VII**, indicating that the structures denoted by their formulations are valid. However, it is difficult to reconcile the ^{11}B NMR spectrum of **IV** with either its solid-state structure or that of its model compound (**XI**). Since the spectrum is broad, it may represent a conglomerate of several different clusters involving $[Na(THF)]^+$ and $[commo\text{-}1,1'\text{-}Mg(2,3\text{-}(SiMe_3)_2\text{-}1,2,3\text{-}MgC_2B_4H_4)_2]^{2-}$. Such extended clusters are known to exist in the THF-solvated natria- and lithiacarboranes.[7]

Acknowledgment. Dedicated with all best wishes to Prof. Heinrich Nöth (Universität Munchen) on the occasion of his 70th birthday. This work was supported by grants from the Robert A. Welch Foundation (Grant Nos. N-1016 and N-1322), the donors of the Petroleum Research Fund, administered by the American Chemical Society, and the National Science Foundation.

Supporting Information Available: Tables of atomic coordinates (Table S-1), a full listing of bond lengths and bond angles (Table S-2), anisotropic displacement parameters (Table S-3), and H-atom coordinates and isotropic displacement coefficients (Table S-4) for **I**, **II**, and **IV** (23 pages). Ordering information is given on any current masthead page.

OM9711133